

A LAPLACE TRANSFORM BASED INVERSE METHOD FOR  
FLAW CHARACTERIZATION BY EDDY CURRENTS

Satish M. Nair and James H. Rose

Center for NDE  
Iowa State University  
Ames, Iowa 50011

INTRODUCTION

Eddy current probes have been widely and successfully used to detect surface breaking flaws in metals. It is quite natural to ask if the eddy current signal can be used to characterize the flaw, i.e. determine its type, length or depth? This paper is a "report in progress" on just this question. The basic strategy is to find an eddy-current flaw characterization problem simple enough that an analytic solution is possible. This analytic solution is then used to uncover the elements generic to eddy-current characterization (inversion) methods.

Such a model has been discussed in last year's report and is now reviewed. Namely we compute the change in impedance of a metallic half-space that contains an arbitrarily shaped inclusion. The inclusion is chosen to have a conductivity nearly the same as the metallic half-space, and the applied magnetic field is chosen to be spatially uniform with its axis parallel to the metal's surface. Since the conductivity is nearly the same everywhere, the induced fields decay nearly exponentially into the metal. Consequently (as was shown), the change in impedance can be written as a Laplace transform of the conductivity variation with depth. Conversely it is found that the conductivity as a function of depth is determined by an inverse Laplace transform of the frequency (time) domain impedance.

Below we very briefly indicate the analytic form of the proposed inversion algorithm. The algorithm is then re-expressed in a form suitable for numerical evaluation. Finally, we present the results of a series of tests on the numerically expressed inversion algorithm. These tests focus on the following items. (1) How well can the algorithm recover various conductivity profile shapes? (2) What is the effect of noise on the inversion? (3) Finally, what happens to the inversion algorithm if the conductivity of the inclusion is not close to that of the host?

An interesting feature of our approach will be remarked on. The inverse problem is formulated in the time-domain. This simplifies the inversion problem significantly since it allows the numerical implementation of the algorithm through the eigenvalues and eigenfunctions of the Laplace Transform.

## IMPEDANCE CHANGE DUE TO INCLUSION

The problem studied is that of a three-dimensional inclusion, surface-breaking or buried, within a metallic halfspace. The magnetic permeability of the inclusion is assumed to be equal to the permeability of the host,  $\mu_0$ . The conductivity of the inclusion is assumed to be  $\sigma_0 + \Delta\sigma(\vec{r})$ , where  $\sigma_0$  is the conductivity of the host. We assume that the materials are linear and isotropic. A uniform magnetic field,  $H_A e^{-i\omega t}$ , arising due to a drive current,  $I$ , is applied on the surface of the halfspace. We then make the approximation that  $\frac{\Delta\sigma}{\sigma_0} \ll 1$  and hence only keep first-order terms in  $\frac{\Delta\sigma}{\sigma_0}$ . This is equivalent to replacing the perturbed fields by their unperturbed values, the so-called Born approximation. Details of the geometry are shown in Fig. 1.

Under such an approximation, it has been shown in [1] that the change in impedance,  $\delta z$ , due to the inclusion is given by

$$\delta z(k_0) \approx \frac{H_A^2}{I^2} \frac{k_0^2}{\sigma_0^2} \int_{-\infty}^{\infty} \int_0^{\infty} \int_{-\infty}^{\infty} \delta\sigma(\vec{r}) e^{2ik_0 y} dx dy dz. \quad (1)$$

$k_0$  is related to the skin depth,  $\beta$ , by  $k_0 = \frac{1+i}{\beta}$ . In terms of the angular frequency,  $\omega$ ,  $k_0 = (1+i)c\omega^{1/2}$  where  $c = \left(\frac{\sigma_0 \mu_0}{2}\right)^{1/2}$ .  $\delta\sigma(\vec{r})$  denotes the conductivity variation within the halfspace and is given by  $\delta\sigma(\vec{r}) = \Delta\sigma(\vec{r}) \Theta(\vec{r})$ .  $\Theta(\vec{r})$  is the characteristic function and is equal to one inside the flaw and zero outside. Denote  $A(y) = \int_{-\infty}^{\infty} \int_{-\infty}^{\infty} \delta\sigma(\vec{r}) dx dz$  as the conductivity profile, representing cross-sections of the conductivity variation at each depth,  $y$ . Then,  $A(y)$  is recovered from its Laplace transform described by

$$\int_0^{\infty} e^{2ik_0 y} A(y) dy = \frac{\delta z(k_0)}{k_0^2} \left[ \frac{H_A^2}{I^2 \sigma_0^2} \right]^{-1} = \bar{G}(k_0). \quad (2)$$

The difficulty in inverting Eq. (2) is that variable  $k_0$  is complex and suitable numerical algorithms are not available. One way to circumvent this difficulty is to switch to the time-domain where all variables will be real. Taking the time-domain Fourier transform of Eq. (1), after some manipulations, we can show that

$$\int_0^{\infty} e^{-su} A(u) du = \frac{s^{-3/2}}{2c^2 \pi} \text{Im} \int_0^{\infty} \frac{\delta z(\omega)}{\omega} \left[ \frac{H_A^2}{I^2 \sigma_0^2 c^2 4\sqrt{\pi}} \right]^{-1} e^{-i\omega 2c^2/s} d\omega = G(s) \quad (3)$$

where  $y^2 = u$  and  $s = 2c^2/t$ . Since the inversion variable "s" is real, Eq. (3) describes a real Laplace transform for which numerical methods have been developed. Therefore, Eq. (3) instead of Eq. (2) is used for the inversion.

Since measurements of the impedance,  $\delta z(\omega)$ , are usually bandlimited, the impedance data needs to be extrapolated, through its low and high frequency asymptotics, to compute the Fourier integrals in Eq. (3). By studying Eq. (2), we see that as  $\omega \rightarrow 0$ ,  $\frac{\delta z(\omega)}{\omega} \rightarrow 0$  ( $\omega^0, \omega^{1/2}, \dots$ ) and when  $\omega \rightarrow \infty$ ,  $\frac{\delta z(\omega)}{\omega} \rightarrow 0$ . The impedance is curvefitted to the corresponding orders of  $\omega$  in the low and high frequency regimes. The contribution to the integrals outside the bandlimits are then estimated analytically.

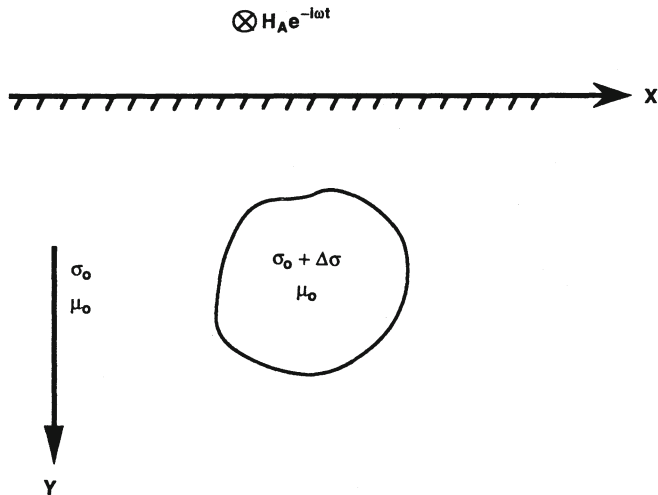


Fig. 1. Description of the inversion problem.

#### NUMERICAL INVERSION OF THE LAPLACE TRANSFORM

The Laplace transform of any arbitrary function,  $A(u)$ , is defined by

$$\int_0^{\infty} e^{-su} A(u) du = G(s), \quad 0 \leq s < \infty \quad (4)$$

provided the integral exists. The Laplace transform is a Fredholm integral equation of the first kind and, as typically happens, is ill-posed (unstable). Details addressing this ill-posedness can be found in Ref. [3-8].

The singular value decomposition (SVD) method has been widely used in solving Fredholm integral equations of the first kind. It provides a convenient method for treating the ill-posedness. When applied to a real Laplace transform, it has been shown that the solution can be written in terms of the eigenvalues and eigenfunctions of the transform [5]. Analytical expressions for these eigenvalues and eigenfunctions are derived in Ref. (5). Using these expressions, we can show that the inversion of a Laplace transform described by Eq. (4) can be written as

$$A(u) = \frac{1}{\pi} \operatorname{Re} \left\{ \int_0^{\infty} d\Omega \frac{u^{-1/2+i\Omega}}{\Gamma(1/2+i\Omega)} \int_0^{\infty} ds G(s) s^{-1/2+i\Omega} \right\}. \quad (5)$$

$\Omega$  is real and unbounded and provides a continuous set of eigenfunctions and eigenvalues for the Laplace transform.  $\Gamma(1/2+i\Omega)$  refers to the complex Gamma function computed for every value of  $\Omega$ . This expression is general in that it describes the inversion of the Laplace transform of any function, provided  $\int_0^{\infty} |A(u)| u^{-1/2} du$  exists. The importance of this equation lies in the fact that it can be implemented numerically without much difficulty or computational costs.

The nature of the ill-posedness can be seen by looking at the outer integral in Eq. (5). As  $\Omega \rightarrow \infty, \Gamma(\frac{1}{2} + i\Omega) \rightarrow 0$ . Since some amount of noise is inevitable (either from computation or from measurement), the outer integral in reality can never be computed to its entirety. We are forced to truncate the outer integral at a value of  $\Omega$ , denoted by  $\Omega_{opt}$ , and to neglect contributions to  $A(u)$  from  $\Omega > \Omega_{opt}$ . This truncation does not pose a problem for smoothly varying profiles. In most NDE situations, smoothed out reconstructions of the flaw profiles suffice, allowing such an approximation to be made.

A procedure to choose the optimum frequency of truncation,  $\Omega_{opt}$ , has been outlined by Lewis in [4]. Two criteria for choosing the optimum frequency are adopted in this paper, one based on finding the minimum error and the second the minimum error slope. We first obtain estimates for  $A$ ,  $A_m(u)$ , from

$$A_m(u) = \frac{1}{\pi} \text{Re} \left\{ \int_0^{\Omega_m} d\Omega \frac{u^{-1/2+i\Omega}}{\Gamma(1/2+i\Omega)} \int_0^\infty ds G(s) s^{-1/2+i\Omega} \right\} \quad (6)$$

for every  $\Omega_m = \Omega_1, \dots, \Omega_{max}$ . This is then substituted back into the forward problem to yield the least square error,  $\bar{R}_m$ , given by

$$\bar{R}_m = \sum_{i=1}^N R_m(s_i) = \sum_{i=1}^N |G(s_i) - \int_0^\infty e^{s_i u} A_m(u) du|^2 \quad (7)$$

Here,  $N$  denotes the total number of points at which  $G(s)$  is measured. In the first criterion,  $(\Omega_{opt})_I$ , is chosen as that frequency among  $\Omega_m = \Omega_1, \dots, \Omega_{max}$  which gives the minimum least square error,  $(\bar{R}_m)_{min}$ . In the second criterion, all the local minima of  $\bar{R}_m$  are located.  $(\Omega_{opt})_{II}$  is then chosen among these minima to be that at which  $\bar{R}_m$  varies the slowest. This is argued from the point of view that at the optimum frequency, insertion or deletion of the next frequency component will not induce large variations in  $A(u)$ .

The inversion algorithm is tested over the Laplace transform of various well known functions. Figures 2 (a) - (c) show results obtained for three different functions, namely,

$$A(u) = \int_0^\infty e^{-su} A(u) du = G(s)$$

$$u e^{-u} \quad 1/(1+s)^2$$

Gaussian Pulse

$$\left( \frac{1}{\sigma\sqrt{2\pi}} e^{-(u-\mu)^2/2\sigma^2} \right) \quad \frac{e^{-u^2/2\sigma^2}}{2} e^{x^2} \text{erfc}(x); \quad x = \frac{\sigma}{\sqrt{2}} \left( s - \frac{\mu}{\sigma^2} \right)$$

Rectangular Pulse

$$= 1, u_1 \leq u \leq u_2 \quad (e^{-su_1} - e^{-su_2})/s$$

$$= 0, \text{ elsewhere}$$

To see how sensitive the recovered solution,  $A(u)$ , is to variations in  $G(s)$ , artificial random noise is added proportionately to  $G(s)$ . The  $N$  in Figures 2 (a) - (c) correspond to the noise factors,  $N = 1\%$  denoting 1% noise and so on. From the figures, we see that the algorithm is able to reconstruct the functions quite well. In the case of the unit square pulse, we are not able to reconstruct exactly the abrupt change in behavior of the profile at  $u = 1$ . Instead, the inversion algorithm seems to smooth this discontinuity so that the function decays slowly. We also see that due to the truncation of the higher frequency components, the algorithm is quite stable to noise, even for magnitudes as large as 10%.

## APPLICATION OF THE INVERSE METHOD

In this section, the problem of a metallic layer over a halfspace is studied. The layer and the halfspace are assumed to have conductivities  $\sigma_1$  and  $\sigma_0$ , respectively. The permeabilities of both are the same,  $\mu_0$ . The layer is assumed to be of thickness 'd'. A uniform field,  $H_A e^{-i\omega t}$ , is applied to the top surface of the layer.

Using Maxwell's equations and by applying appropriate boundary conditions at  $y=0, y=d$ , and  $y=\infty$ , the fields within the layer and halfspace are obtained. These are then substituted into the reciprocity relation in [9] to compute the impedance change caused by the presence of the layer. This is given as

$$\delta z = \frac{H_A^2}{I^2} \frac{ik_0}{\sigma_0} \left[ 1 - \left( \frac{\sigma_0}{\sigma_1} \right)^{1/2} \frac{e^{-2ik_1 d} F + 1}{e^{-2ik_1 d} F - 1} \right] \quad (8)$$

where

$$F = \frac{1 + (\sigma_0/\sigma_1)^{1/2}}{1 - (\sigma_0/\sigma_1)^{1/2}}, \quad k_1^2 = i\omega\mu_0\sigma_1, \quad \text{and} \quad k_0^2 = i\omega\mu_0\sigma_0.$$

The impedance is computed for various ratios of  $\sigma_1/\sigma_0$  for frequencies ranging from  $\frac{\omega}{\beta} = 0.1$  to 5. These are then inverted through Eq. (5) to recover the conductivity profile of the layered solid. Figures 3 (a) - (c) show the profiles reconstructed from the inversion. The dashed line in each figure represents the actual profile. Instead of truncating at  $\Omega_{opt}$  and neglecting higher frequency contributions, a weighting function of the form  $w(\Omega) = 1/(1 + e^{\alpha(\Omega - \Omega_{opt})})$  is used.  $\alpha$  here is a weighting coefficient. When  $\alpha = \infty$ ,  $w = 1$  for  $\Omega < \Omega_{opt}$  and zero elsewhere, thus representing a rectangular window. Each figure shows two reconstructed profiles, one with a rectangular window and one with parameter  $\alpha = 2$ . It is expected that  $\alpha = 2$  will smooth out the oscillations in the recovered profiles and provide a much better reconstruction.

From Figures 3 (a) - (c), as expected, we see that as the ratio of  $\sigma_1/\sigma_0$  increases, the reconstruction of the layer profile worsens gradually. The algorithm gives accurate estimates of the profiles for disparities in conductivities up to about 10%. Even, beyond that range, the reconstructed profiles behave very similar to the actual profiles and a reasonable estimate of the depth of the layer can be made. This is clearly brought out in Fig. 3 (c) where the conductivity of the layer is twice that of the host.

Impedance values are usually contaminated with noise, filtering in from experimental measurements. The sensitivity of the algorithm to noise in the impedance hence needs to be studied. Once again, as in the previous section, random noise is added proportionately to the impedance. From the results, as shown in Figures 4 (a) and (b), it is found that the reconstructed profiles compare well with actual solutions, even when the noise is as large as 10% of the computed impedance values. It is however seen that the data needs to be smoothed prior to inversion to provide meaningful solutions.

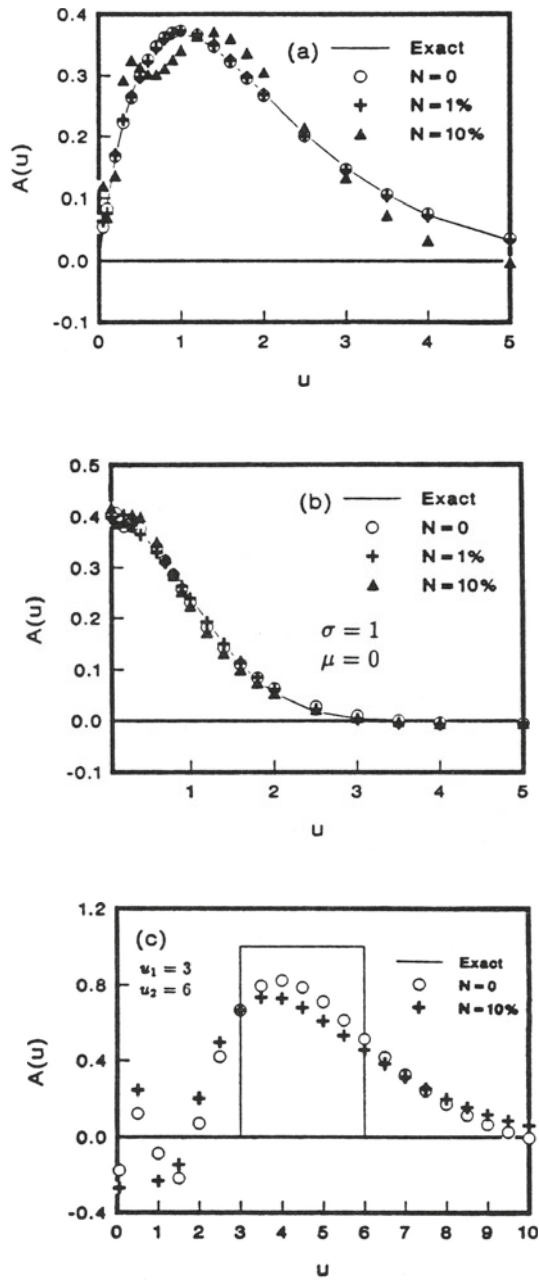


Fig. 2. Inversion of Laplace transform (a)  $A(u) = ue^{-u}$  (b)  $A(u) =$  Gaussian Pulse (c)  $A(u) =$  Rectangular pulse.

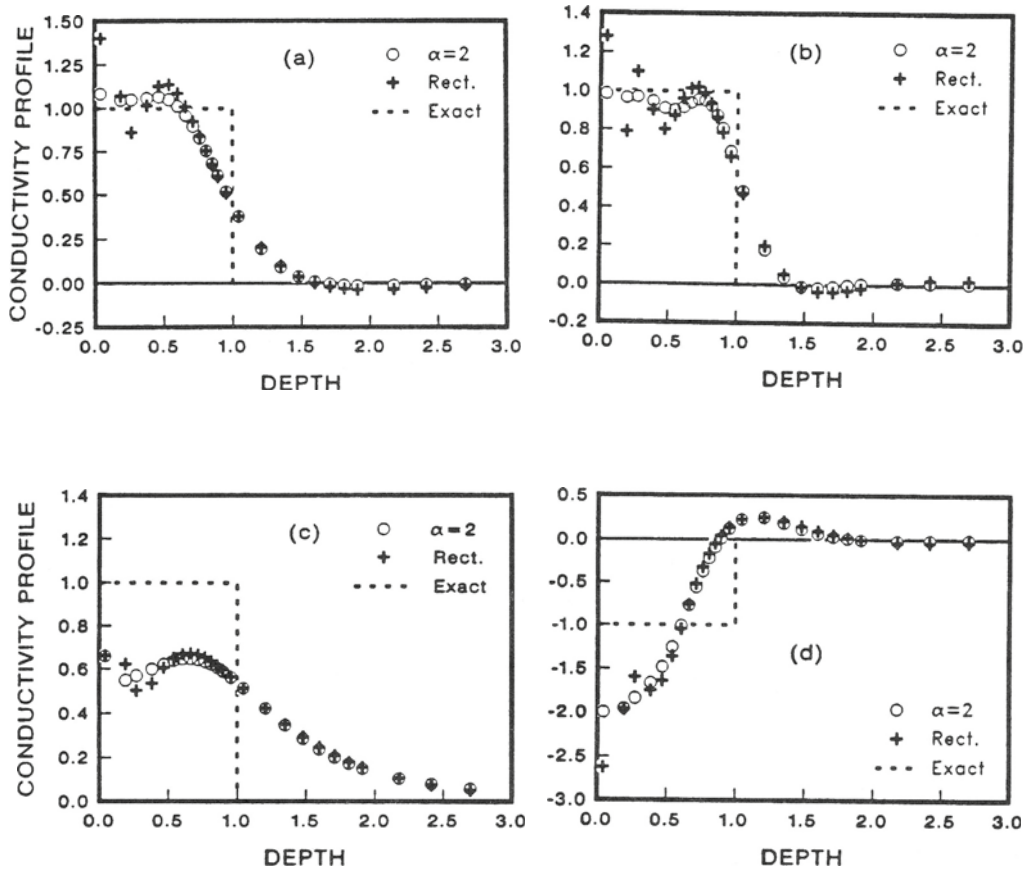


Fig. 3. Reconstruction of layer profile ( $\Delta\sigma/|\Delta\sigma|_{\text{actual}}$ ) for  
 (a)  $\sigma_1/\sigma_0 = 1.01$ , (b)  $\sigma_1/\sigma_0 = 1.1$  (c)  $\sigma_1/\sigma_0 = 2.0$  (d)  $\sigma_1/\sigma_0 = 0.5$ .

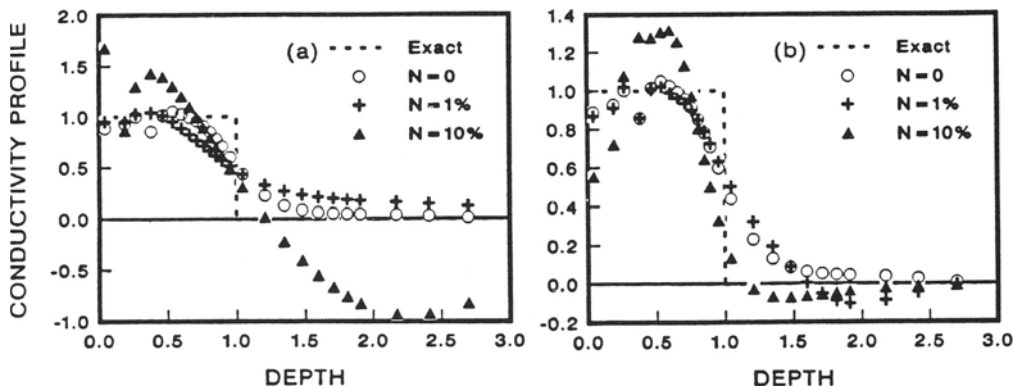


Fig. 4. Reconstruction of layer profile in the presence of noise and for  $\sigma_1/\sigma_0 = 1.1$ . (a) unsmoothed (b) smoothed.

#### CONCLUSIONS

In this paper, we report the partial development of an inversion algorithm for the characterization of inclusions within a metallic halfspace. The algorithm requires the numerical inversion of a Laplace transform. The algorithm is tested by using it to reconstruct conductivity profiles of a metallic layer over a halfspace. The present partial formulation of the problem allows us to recover the flaw's conductivity as a function of depth. Work is in progress to extend the method so that it will be possible to recover the entire conductivity profile of the flaw.

#### ACKNOWLEDGMENT

This work was supported by the Center for NDE at Iowa State University and was performed at the Ames Laboratory. Ames Laboratory is operated for the U. S. Department of Energy by Iowa State University under Contract No. W-7405-ENG-82.

#### REFERENCES

1. S. M. Nair, J. H. Rose, and V. G. Kogan, in Review of Progress in Quantitative NDE, edited by D. O. Thompson and D. E. Chimenti, (Plenum Press, New York, 1988), Vol. 7A, pp. 461-469.
2. B. Davies and B. Martin, *Journal of Computational Physics*, 33, 1-32, (1979).
3. C. T. H. Baker, L. Fox, D. F. Mayers, and K. Wright, *Computational Journal*, 7, 141-148 (1964).
4. B. A. Lewis, *J. Inst. Math. Applics.* 16, 207-220 (1975).
5. J. G. McWhirter and E. R. Pike, *J. Phys. A. Math. Gen.*, Vol. 11, No. 9, 1729-1745 (1978).
6. A. N. Tihonov, *Soviet Math. Dokl.* 4, 1035-1038 (1963).
7. G. F. Miller in Numerical Solution of Integral Equations, 1st edition, edited by L. M. Delves and J. Walsh (Oxford University Press, Oxford, 1974), Ch. 13.
8. L. M. Delves and J. L. Mohammed, Computational Methods for Integral Equations, (Cambridge University Press, Cambridge, 1985).
9. B. A. Auld, F. G. Muennemann, and M. Riazat, in Research Techniques in Nondestructive Testing, Vol. 7, edited by R. S. Sharpe (Academic Press, London, 1984), Ch. 2.